This paper is published as part of a *PCCP* themed issue on dynamic nuclear polarization

Guest Editors: Robert Griffin and Thomas Prisner

Editorials

High field dynamic nuclear polarization—the renaissance
R. G. Griffin and T. F. Prisner, *Phys. Chem. Chem. Phys.*, 2010, **12**, 5737
http://dx.doi.org/10.1039/c0cp90019b

The discovery and demonstration of dynamic nuclear polarization—a personal and historical account
Charles P. Slichter, *Phys. Chem. Chem. Phys.*, 2010, **12**, 5741
http://dx.doi.org/10.1039/c003286g

Communications

High power pulsed dynamic nuclear polarisation at 94 GHz
Robert I. Hunter, Paul A. S. Cruickshank, David R. Bolton, Peter C. Riedi and Graham M. Smith, *Phys. Chem. Chem. Phys.*, 2010, **12**, 5752
http://dx.doi.org/10.1039/c002251a

Papers

DNP enhanced NMR using a high-power 94 GHz microwave source: a study of the TEMPOL radical in toluene
Eugeny V. Kryukov, Mark E. Newton, Kevin J. Pike, David R. Bolton, Radoslaw M. Kowalczyk, Andrew P. Howes, Mark E. Smith and Ray Dupree, *Phys. Chem. Chem. Phys.*, 2010, **12**, 5757
http://dx.doi.org/10.1039/c003189e

Rapid sample injection for hyperpolarized NMR spectroscopy
Sean Bowen and Christian Hilty, *Phys. Chem. Chem. Phys.*, 2010, **12**, 5766
http://dx.doi.org/10.1039/c002316g

Slice-selective single scan proton COSY with dynamic nuclear polarisation
Rafal Panek, Josef Granwehr, James Leggett and Walter Köckenberger, *Phys. Chem. Chem. Phys.*, 2010, **12**, 5771
http://dx.doi.org/10.1039/c002710n

Prospects for sub-micron solid state nuclear magnetic resonance imaging with low-temperature dynamic nuclear polarization
Kent R. Thurber and Robert Tycko, *Phys. Chem. Chem. Phys.*, 2010, **12**, 5779
http://dx.doi.org/10.1039/c0cp00157k

Liquid state DNP using a 260 GHz high power gyrotron
Vasyl Denysenkov, Mark J. Prandolini, Marat Gafurov, Deniz Sezer, Burkhard Endeward and Thomas F. Prisner, *Phys. Chem. Chem. Phys.*, 2010, **12**, 5786
http://dx.doi.org/10.1039/c003697h

Exploring the limits of electron-nuclear polarization transfer efficiency in three-spin systems
Nikolas Pomplun and Steffen J. Glaser, *Phys. Chem. Chem. Phys.*, 2010, **12**, 5791
http://dx.doi.org/10.1039/c003751f

Dynamic nuclear polarization experiments at 14.1 T for solid-state NMR
Yoh Matsuki, Hiroki Takahashi, Keisuke Ueda, Toshitaka Idehara, Isamu Ogawa, Mitsuru Toda, Hideo Akutsu and Toshimichi Fujiwara, *Phys. Chem. Chem. Phys.*, 2010, **12**, 5799
http://dx.doi.org/10.1039/c002268c

Trityl biradicals and ^{13}C dynamic nuclear polarization
Sven Macholl, Haukur Jóhannesson and Jan Henrik Ardenkjaer-Larsen, *Phys. Chem. Chem. Phys.*, 2010, **12**, 5804
http://dx.doi.org/10.1039/c002699a

Feasibility of *in vivo* ^{15}N MRS detection of hyperpolarized ^{15}N labeled choline in rats
Cristina Cudalbu, Arnaud Comment, Fiodar Kurdzesau, Ruud B. van Heeswijk, Kai Uffmann, Sami Jannin, Vladimir Denisov, Deniz Kirik and Rolf Gruetter, *Phys. Chem. Chem. Phys.*, 2010, **12**, 5818
http://dx.doi.org/10.1039/c002309b

Polychlorinated trityl radicals for dynamic nuclear polarization: the role of chlorine nuclei
Juan Carlos Paniagua, Verónica Mugnaini, Cristina Gabellieri, Miguel Feliz, Nans Roques, Jaume Veciana and Miquel Pons, *Phys. Chem. Chem. Phys.*, 2010, **12**, 5824
http://dx.doi.org/10.1039/c003291n

Shuttle DNP spectrometer with a two-center magnet
Alexander Krahn, Philip Lottmann, Thorsten Marquardsen, Andreas Tavernier, Maria-Teresa Türke, Marcel Reese, Andrei Leonov, Marina Bennati, Peter Hoefer, Frank Engelke and Christian Griesinger, *Phys. Chem. Chem. Phys.*, 2010, **12**, 5830
http://dx.doi.org/10.1039/c003381b

Properties of dinitroxides for use in dynamic nuclear polarization (DNP)
Cédric Ysacco, Egon Rizzato, Marie-Alice Virolleaud, Hakim Karoui, Antal Rockenbauer, François Le Moigne, Didier Siri, Olivier Ouari, Robert G. Griffin and Paul Tordo, *Phys. Chem. Chem. Phys.*, 2010, **12**, 5841
http://dx.doi.org/10.1039/c002591g

Feasibility of *in vivo* ^{15}N MRS detection of hyperpolarized ^{15}N labeled choline in rats

Cristina Cudalbu,*[a] Arnaud Comment,[abc] Fiodar Kurdzesau,[bd] Ruud B. van Heeswijk,[a] Kai Uffmann,[a] Sami Jannin,[b] Vladimir Denisov,[e] Deniz Kirik[e] and Rolf Gruetter[acf]

Received 2nd February 2010, Accepted 23rd April 2010
First published as an Advance Article on the web 12th May 2010
DOI: 10.1039/c002309b

The increase of total choline in tumors has become an important biomarker in cancer diagnosis. Choline and choline metabolites can be measured *in vivo* and *in vitro* using multinuclear MRS. Recent *in vivo* ^{13}C MRS studies using labeled substrates enhanced *via* dynamic nuclear polarization demonstrated the tremendous potential of hyperpolarization for real-time metabolic studies. The present study demonstrates the feasibility of detecting hyperpolarized ^{15}N labeled choline *in vivo* in a rat head at 9.4 T. We furthermore report the *in vitro* (172 ± 16 s) and *in vivo* (126 ± 15 s) longitudinal relaxation times. We conclude that with appropriate infusion protocols it is feasible to detect hyperpolarized ^{15}N labeled choline in live animals.

1. Introduction

Many magnetic resonance spectroscopy (MRS) studies of choline metabolism have shown increased levels of total Cho (tCho) in cancers developing in different organs, such as brain,[1–5] prostate[6–8] and breast.[9–13] The increase of tCho in tumors has become a potentially important biomarker in cancer diagnosis.[14–16] Recent results have shown a significant decrease of tCho concentration in breast cancers responding to chemotherapy.[17] Overall, there is strong evidence suggesting the importance of this biomarker in monitoring the response to different treatments such as radiotherapy, chemotherapy or brachytherapy.[17–20]

Cho penetrates cell membranes and is a natural constituent of blood.[21] In addition, Cho is a precursor of various metabolic pathways. In the brain, for example, choline is a substrate of choline containing phospholipids and of acetylcholine.[22,23] However, in tumors Cho is integrated mainly into phospholipids,[21,22] a major constituent of cell membranes. Cho is incorporated into cell membranes by adenosine triphosphate (ATP) dependent phosphorylation and transformed by choline kinase in phosphocholine (PCho). Then, PCho is activated by the reaction with cytidine triphosphate forming cytidine diphosphate (CDP)-choline. Through phosphocholine transferase, PCho is transferred from CDP-choline producing phosphatidylcholine and cytidine monophosphate.

Although PET data reported that choline uptake into the healthy brain is considered to be low relative to other organs (kidney, liver, *etc.*),[22,23] Klein *et al.*[24–26] reported that free choline is present in minute amounts in the brain, with a Cho arterial-venous difference of max 88.6 μM corresponding to an uptake of 70 nmol g^{-1} of brain per minute. Normal brain cells do not need much Cho for cell membrane formation because they are in a non-dividing postmitotic state.[22] Conversely, increased cell membrane synthesis is present in brain tumors. Hara *et al.*[23] indeed observed high ^{11}C choline uptake in brain tumors. In addition, Shinoura *et al.*[22] acquired PET data 5 min after ^{11}C Cho injection, showing incorporation of ^{11}C Cho into human brain tumors within 5 min. This high Cho uptake in tumors is consistent with MRS measurements, in which elevated concentrations of tCho were found in brain tumors.[1–5]

Choline and choline metabolites can be measured *in vivo* and *in vitro*, in different organs and in cells using multinuclear MRS. Proton MRS is a wildly used technique to investigate the tCho amounts in different organs both *in vivo* and *in vitro*. The tCho signal, which is detected by ^{1}H MRS at ~3.2 ppm represents a combination of three signals: free choline, PCho and glycerophosphocholine. Phosphorus MRS is another option for detecting ^{31}P-containing choline compounds. In addition, it is also feasible to label choline nuclei with *e.g.* ^{13}C, ^{2}H and ^{15}N and then monitor the incorporation of the label into choline metabolites.[27] However, the low natural abundance of *e.g.* ^{15}N (0.365%) makes the study of nitrogen metabolism difficult. The study of nitrogen metabolism by ^{15}N MRS requires the continuous infusion for several hours of a ^{15}N labeled substrate.[28,29] The recently developed hyperpolarization technique based on dynamic nuclear polarization[30] opened new perspectives for metabolic studies using heteronuclei since the NMR signal-to-noise ratio is enhanced by up to four

[a] *Laboratory for Functional and Metabolic Imaging, Ecole Polytechnique Fédérale de Lausanne, EPFL-SB-IPMC-LIFMET, Office F1 602, Station 6, CH-1015 Lausanne, Switzerland. E-mail: cristina.cudalbu@epfl.ch; Fax: +41-21-693-7960; Tel: +41-21-693-0580*
[b] *Institute of Condensed Matter Physics, Ecole Polytechnique Fédérale de Lausanne, Lausanne, Switzerland*
[c] *Department of Radiology, University of Lausanne, Switzerland*
[d] *Paul Scherrer Institute, Villigen, Switzerland*
[e] *Department of Experimental Medical Science, Brain Repair and Imaging in Neural Systems (BRAINS), Lund University, Lund, Sweden*
[f] *Department of Radiology, University of Geneva, Switzerland*

orders of magnitude.[31] The main limitation of the technique is that *in vivo* studies are only possible on nuclei with long longitudinal relaxation times (T_1), and so far carboxyl ^{13}C nuclei (*e.g.* pyruvate, acetate and bicarbonate) have been the most promising candidates.[32–35] Previous studies have shown the utility of this technique for detecting *in vivo* tumors in animal models[36,37] and very low contrast agent concentrations.[38] To date, besides optically polarized ^{3}He and ^{129}Xe,[39] ^{6}Li is the only hyperpolarized nucleus besides ^{13}C that has been reported to be detected *in vivo*.[38] Two recent studies reported remarkably long *in vitro* longitudinal relaxation times for ^{15}N Cho,[40,41] suggesting that hyperpolarized ^{15}N Cho could be a suitable candidate for *in vivo* experiments.

However, the rapid bolus administration of Cho requires an approach compatible with its toxicity to lungs and mucous membrane. To our knowledge the *in vivo* detection of hyperpolarized ^{15}N Cho has not been demonstrated to date and we report here the first *in vivo* study using DNP-enhanced ^{15}N nuclei.

The aim of the present study was twofold: (1) to demonstrate the feasibility of detecting DNP-enhanced ^{15}N labeled Cho *in vivo* in a rat head and (2) to measure T_1 relaxation times *in vivo*.

2. Results and discussion

The time evolution of the ^{15}N solid-state polarization was measured at 1.2 K using a dedicated home-built NMR spectrometer and a remotely tuned and matched low-temperature NMR probe.[42] The polarization time constant was 2700 ± 200 s. Fig. 1 shows an example of a representative ^{15}N Cho polarization curve. The ^{15}N solid-state polarization was enhanced by DNP for 2.5 h prior to performing the dissolution step. The maximum solid-state polarization was measured to be 3.3 ± 0.3%. This value, which was confirmed by the comparison between the liquid-state thermal equilibrium signal intensity and the hyperpolarized signal measured immediately after dissolution, corresponds to a signal enhancement of 10 000 ± 900 if compared to the room-temperature thermal equilibrium signal in a field of 9.4 T. Nearly the same enhancement factor was reported by Gabellieri *et al.*[41] at 9.4 T, using a commercial DNP polarizer working at 3.35 T and 1.4 K with trityl radicals as polarizing agent.

As can be seen in Fig. 2, the *in vitro* ^{15}N Cho signal remained visible for ~800–900 s. Taking into account RF pulse effects, the apparent *in vitro* T_1 was estimated to be 172 ± 16 s (n = 4). The correlation coefficients were between 0.91–0.99.

Due to the toxicity of Cho to lungs and mucous membrane, it was necessary to determine the maximum concentration that can be infused while maintaining the animal within normal physiological ranges. This was established in bench experiments designed to simulate the injection performed in the rat by the external pump immediately after the DNP dissolution (2.5 ml injected into the rat femoral vein over 9 s). At concentrations of ~90 mM, the rats remained physiologically stable allowing at least two subsequent injections on the same animal.

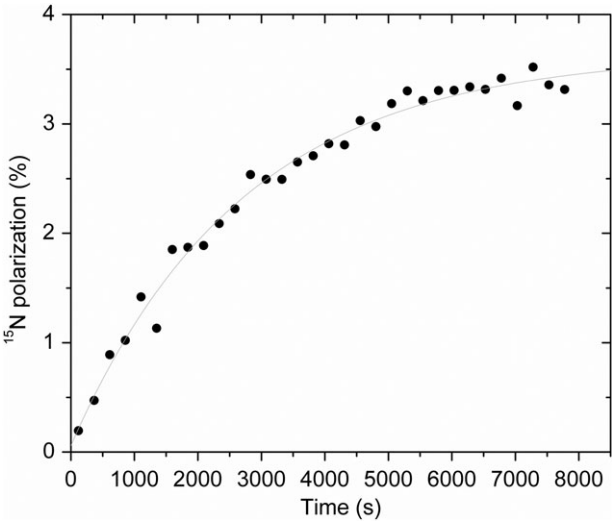

Fig. 1 ^{15}N polarization curve recorded at 1.2 K prior to dissolution using 5 degree RF pulses. The build-up time constant was 2700 ± 200 s and the polarization prior to dissolution was 3.3 ± 0.3%.

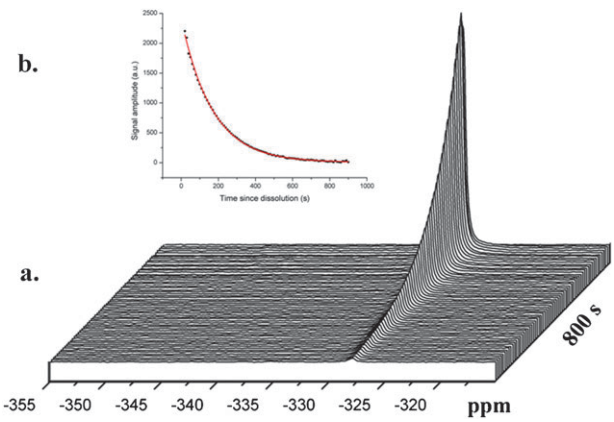

Fig. 2 (a) Series of spectra of hyperpolarized *in vitro* ^{15}N Cho measured in a phantom. The signal is visible up to ~800–900 s after dissolution. Individual spectra were processed with 10 Hz Lorentzian line broadening. The ^{15}N chemical shifts were referenced to nitromethane. (b) Decay curve of the same *in vitro* signal amplitudes (black dots) corrected for the RF flip angle effects. The fit of the plotted decay curve is also shown (line).

Fig. 3 displays a series of *in vivo* spectra of hyperpolarized ^{15}N Cho. The *in vivo* ^{15}N Cho signal was discernible above the noise level for ~100 s despite the repeated RF pulsing at 10°, with *in vivo* linewidths of 9 ± 2 Hz. The characteristic *in vivo* T_1 was 126 ± 15 s (n = 5), after correcting for RF flip angle effects. The correlation coefficients were between 0.91–0.99. The *in vivo* signal-to-noise ratio (SNR) was approximately 10-fold lower compared to the *in vitro* experiments, as a consequence of the lower Cho concentration in the sensitive volume of the coil.

The present study demonstrates for the first time the feasibility of detecting hyperpolarized ^{15}N labeled Cho *in vivo* in a rat head. Hyperpolarized ^{15}N Cho was administrated two consecutive times to the same animal at a concentration of ~90 mM, showing that hyperpolarized ^{15}N Cho can be administered and subsequently detected *in vivo*.

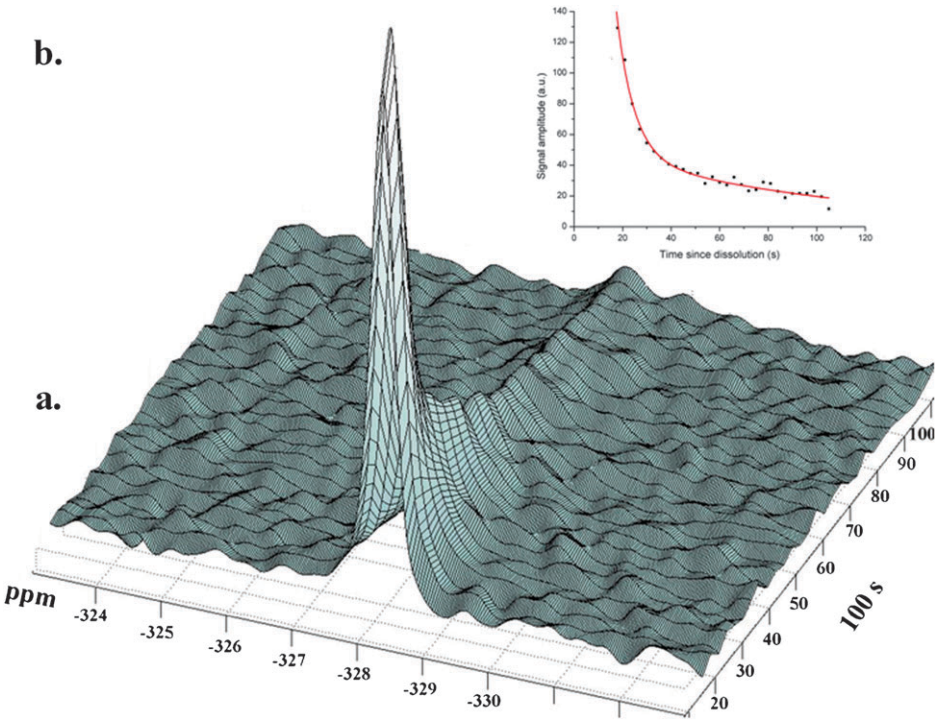

Fig. 3 (a) Plot of the first 31 *in vivo* ^{15}N Cho spectra over time. Individual spectra were processed with 10 Hz Lorentzian line broadening. The ^{15}N chemical shifts were referenced to nitromethane. (b) Decay curve of the same *in vivo* signal amplitudes (black dots) corrected for RF flip angle effects. The fit of the plotted decay curve is also shown (line).

We furthermore report the *in vitro* and *in vivo* longitudinal relaxation times at 9.4 T. Our *in vitro* results in a phantom (T_1 = 172 ± 16 s) were in good agreement with the *in vitro* values of 189 ± 2 s and 203 ± 10 s reported in previous ^{15}N hyperpolarized Cho studies performed in high-resolution NMR systems.[40,41]

In vivo relaxation times showed a decrease compared with the *in vitro* values, which can be explained by the fact that the relaxation times of metabolite are likely to be influenced by the microenvironment.[43] In addition, the *in vivo* relaxation times exhibited a deviation from the standard mono-exponential decay, with a very fast decay (6 ± 1.5 s) during the first seconds, followed by a slower decay afterwards (126 ± 15 s). This was very unlikely due to the presence of TEMPO, which can act as a relaxing agent within the first seconds, since this was not observed *in vitro*. Effects related to the presence of deoxygenated and oxygenated blood are also unlikely to be the cause, since the bolus passes first through the heart and thereafter to the lungs where it becomes oxygenated before it reaches the brain. It is also unlikely that instability issues in the first seconds after the injection related to the animal reaction to the bolus shorten the T_1 since during bench and MR experiments animals were behaving normally. Therefore, the bi-exponential decay likely reflects the presence of Cho first in the blood and afterwards in the brain due to uptake. By infusing 90 mM of Cho into the femoral vein, the Cho concentration into the blood is estimated at ~5 μmol ml^{-1} (blood and interstitial volume of 10% of the body weight, http://www.ahc.umn.edu/rar/BLOOD.HTML). Considering a cerebral blood volume of ~3%,[44] the apparent tissue Cho concentration would amount to a signal originating from an apparent tissue concentration of ~150 nmol g^{-1} (specific weight of ~1 g ml^{-1}). An uptake of 70 nmol g^{-1} of brain min^{-1} has been reported,[24–26] consequently after ~40 s we should have (neglecting efflux) ~50 nmol g^{-1} of Cho in the brain, which represents one-third of the observed Cho signal. From these considerations it appears likely that a significant fraction of the Cho signal arises from the cerebral compartment, in addition to the blood pool. Further investigations have to be performed in order to precisely assess the amount of the MRS choline signal originating from brain and from the blood pool.

Although Cho uptake into the healthy brain is considered to be lower relative to the uptake of other organs,[22,23] it is of interest to note that all ^{11}C Cho PET studies imaging brain tumors showed a very high uptake of ^{11}C Cho in brain tumors. Compared to ^{15}N choline, ^{11}C choline has a half-life of ~20 min and the dose injected in rats is ~0.2 ml (0.3–0.4 GBq).[22] However, recent studies have shown that ^{15}N in deuterated choline[40] has a lifetime of only 3 times less than that of ^{11}C-choline. In addition, our data suggest that with an uptake of 70 nmol g^{-1} of brain min^{-1} [24–26] it is very possible that a sufficient fraction of Cho enters the brain, so that it becomes detectable before the *in vivo* hyperpolarized ^{15}N Cho signal disappears in the noise (*i.e.* within a time window of about 100 s). Consequently, since total Cho becomes an important biomarker in cancer diagnosis, the long T_1 obtained in our study combined with the potential to observe hyperpolarized ^{15}N Cho *in vivo* makes this compound useful for early detection of tumors. Thus, hyperpolarized ^{15}N Cho could become an alternative MR technique to PET imaging with ^{11}C choline. Moreover, due to the long *in vivo* T_1, ^{15}N Cho could be used to

detect very low contrast agent concentrations, as has been shown previously for ^{6}Li by van Heeswijk *et al.*[38] Hyperpolarized ^{15}N Cho could also be potentially used in the assessment of blood flow.

For a given and equal polarization, the SNR should be about 2.5 times smaller for ^{15}N than for ^{13}C since it should be proportional to the gyromagnetic ratio times the nuclear polarization if the main source of noise in the experiment is originating from the sample, as is the case for most MR experiments in fields above 1T.[45] At a given time, the SNR depends on the longitudinal relaxation time, which was in the present *in vivo* ^{15}N study on the order of $\sim$5 times longer than the typical ^{13}C characteristic decays observed *in vivo*.[46,47] Therefore, despite the lower sensitivity of nitrogen, its longer decay time should allow to probe biological processes on an extended time scale. The relatively long T_1 of ^{15}N may render other nitrogen compounds suitable for DNP-enhanced *in vivo* metabolic studies. ^{15}N MRS labeled experiments are particularly useful for measuring the rates of synthesis of amino acids such as glutamate and glutamine, implicated in glutamate neurotransmission.[28,29]

3. Experimental

Dissolution DNP

For the hyperpolarization of ^{15}N Cho, 98% ^{15}N enriched choline chloride (Sigma Aldrich, St. Louis, MO) solution was prepared at a concentration of 6 M in a 60/40 v/v deuterated water/glycerol solvent doped with 50 mM of TEMPO (2,2,6,6-tetramethyl-1-piperidinyloxy, 98% purity, Sigma-Aldrich, St. Louis, MO) as polarizing agent. This solution was polarized at 3.35 T and 1.2 K using a custom-built polarizer described by Comment *et al.*[35,48] The output power of the 94 GHz microwave source was set to 30 mW. After dissolution into 5 ml of superheated D_2O pressurized at 10 bars, the solution was automatically transferred within 4 s to a phase separator/infusion pump placed in the bore of the 9.4 T system positioned approximately 4 m away from the DNP polarizer. An external pump subsequently drove the injection of 2.5 ml of the hyperpolarized solution into the rat femoral vein over 9 s. The concentration of the ^{15}N Cho infusate was $\sim$90 mM. This concentration corresponds to the maximum concentration that can be infused while maintaining the animal within normal physiological ranges. It was determined through bench experiments with non-hyperpolarized and non-labeled Cho solution using the infusion system designed for the DNP experiments. At least two consecutive injections of hyperpolarized ^{15}N Cho separated by a delay of 3 h could be performed on the same animal. Note that the residual radicals (about 0.8 mM) were not filtered out of the hyperpolarized solution. TEMPO is however known to have low toxicity[49] and nitroxyl radicals are in fact used as *in vivo* antioxidants.[50–52]

Animals

All animal experiments were conducted according to federal and local ethical guidelines and the protocols were approved by the local regulatory body.

For the *in vivo* experiments, male Sprague-Dawley rats (n = 5, $\sim$400 g) were anesthetized using 1.5% isoflurane. One femoral vein and one artery were cannulated for ^{15}N choline chloride injection and blood sampling (monitoring blood gases and pH), respectively. Approximately 0.1 ml of blood was used to measure physiological parameters with an AVL Compact 3 pH/blood gas analyzer (Roche Diagnostics GmbH, Germany). The pH and blood gases were maintained within normal physiological ranges (mean pH $\pm$ SD = 7.31 $\pm$ 0.04; mean pCO2 $\pm$ SD = 43.5 $\pm$ 1.8). During the MRS experiments, respiration rate and blood pressure were monitored using a small-animal monitoring system (SA Instruments Inc., New York, NY, USA) and maintained within a normal range. Body temperature was measured using a rectal thermosensor and maintained at 38.0 $\pm$ 0.5 °C by circulating warm water through tubes around the animal. The physiological parameters remained within normal physiological ranges after the choline bolus injection. During the bolus injection the respiration rate slowed down by $\sim$ 10%, but recovered to normal in the next few minutes.

^{15}N MRS

In vitro and *in vivo* ^{15}N spectra were measured on a Varian Inova spectrometer (Palo Alto, Ca, USA) interfaced to an actively-shielded 9.4 Tesla magnet (Magnex Scientific, Oxford, UK) with a 31 cm horizontal bore and 12 cm id gradient sets giving a maximum gradient strength of 400 mT m^{-1} in 120 μs. A home-built 14 mm diameter ^{1}H quadrature surface coil combined with a 5 loops-10 mm diameter ^{15}N surface coil placed on the head of the animal was used for transmission and reception. A time dependent quantitative eddy current field mapping[53] was used for eddy currents minimization. First and second-order shims were adjusted using FASTESTMAP.[54] Images for localization were obtained in the coronal plane using a multislice fast spin echo sequence with TE/TR = 60/5000 ms, slice thickness = 1 mm, FOV = 25 × 25 mm, matrix = 256 × 256 and 2 averages. The *in vitro* and *in vivo* acquisitions were performed using a 3 ms 10° BIR4 pulse[55] with 10 and 3 s interpulse delay, respectively. The scanning time of the *in vivo* MRS experiment was 600 s (200 acquisitions with TR = 3 s). The ^{15}N *in vivo* and *in vitro* signals were fitted using AMARES (advanced method for accurate, robust, and efficient spectral fitting)[56] from the jMrui software.[57] The signals were Lorentzian line broadened with 10 Hz, one Lorentzian spectral component was selected to fit the major contribution of the metabolite, the zero-order phase was estimated and the first-order phase was fixed to zero for each signal of the time series. The accuracy of the amplitude estimates was assessed using the Cramér-Rao lower bounds.[58] Then, the *in vitro* and *in vivo* longitudinal relaxation times were determined from the hyperpolarized signal decay corrected for the magnetization loss due to the RF excitations by dividing the signal amplitude after the nth excitation pulse by $\cos(10^\circ)^{n-1}$, where n represents the number of excitations. The correlation coefficients reflecting the quality of the least squares fit *vs.* the original data were computed for each fit. A typical standard error of the fitted T_1 was about 5%.

4. Conclusion

We conclude that with appropriate infusion protocols it is feasible to detect hyperpolarized ^{15}N labeled Cho in live animals. To the best of our knowledge, the present manuscript reports the first *in vivo* detection of a DNP-enhanced ^{15}N-substrate. The generally long longitudinal relaxation times of ^{15}N nuclear spins that are not directly bound to protons make these nuclei very attractive for *in vivo* applications using hyperpolarized biomolecules.

Acknowledgements

We are deeply grateful to Dr Jacques van der Klink for initiating the DNP projects in Lausanne and for his invaluable technical help. The authors thank Dr V Mlynarik, Dr C Perazzolo, the veterinary team of CIBM (Dr Hanne Frenkel, Stéphane Germain, Dr Agathe Python) and the RF team (Yves Pilloud, Dr A Magill) for the precious help. This work was supported by the Centre d'Imagerie BioMédicale (CIBM) of the UNIL, UNIGE, HUG, CHUV, EPFL; by the Leenards and Jeantet Foundations; by the Swiss National Science Foundation grant 200020_129901, grant 3100A0-116220; by the EU grant MRTN-CT-2006-035801; and by the National Competence Center in Biomedical Imaging (NCCBI).

References

1 P. B. Barker, J. D. Glickson and R. N. Bryan, *Top. Magn. Reson. Imaging*, 1993, **5**, 32–45.
2 P. J. Pouwels and J. Frahm, *Magn. Reson. Med.*, 1998, **39**, 53–60.
3 B. Ross and T. Michaelis, *Magn. Reson. Q*, 1994, **10**, 191–247.
4 W. Moller-Hartmann, S. Herminghaus, T. Krings, G. Marquardt, H. Lanfermann, U. Pilatus and F. E. Zanella, *Neuroradiology*, 2002, **44**, 371–381.
5 F. A. Howe and K. S. Opstad, *NMR Biomed.*, 2003, **16**, 123–131.
6 P. Narayan and J. Kurhanewicz, *Prostate*, 1992, **21**(s4), 43–50.
7 F. Schick, H. Bongers, S. Kurz, W. I. Jung, M. Pfeffer and O. Lutz, *Magn. Reson. Med.*, 1993, **29**, 38–43.
8 J. Kurhanewicz, D. B. Vigneron, H. Hricak, P. Narayan, P. Carroll and S. J. Nelson, *Radiology*, 1996, **198**, 795–805.
9 K. Glunde, C. Jie and Z. M. Bhujwalla, *Neoplasia*, 2006, **8**, 758–771.
10 M. A. Jacobs, P. B. Barker, P. A. Bottomley, Z. Bhujwalla and D. A. Bluemke, *J. Magn. Reson. Imaging*, 2004, **19**, 68–75.
11 D. K. Yeung, H. S. Cheung and G. M. Tse, *Radiology*, 2001, **220**, 40–46.
12 J. R. Roebuck, K. M. Cecil, M. D. Schnall and R. E. Lenkinski, *Radiology*, 1998, **209**, 269–275.
13 N. R. Jagannathan, M. Singh, V. Govindaraju, P. Raghunathan, O. Coshic, P. K. Julka and G. K. Rath, *NMR Biomed.*, 1998, **11**, 414–422.
14 K. Glunde and N. J. Serkova, *Pharmacogenomics*, 2006, **7**, 1109–1123.
15 K. Glunde, M. A. Jacobs and Z. M. Bhujwalla, *Expert Rev. Mol. Diagn.*, 2006, **6**, 821–829.
16 K. Glunde, E. Ackerstaff, N. Mori, M. A. Jacobs and Z. M. Bhujwalla, *Mol. Pharmaceutics*, 2006, **3**, 496–506.
17 S. Meisamy, P. J. Bolan, E. H. Baker, R. L. Bliss, E. Gulbahce, L. I. Everson, M. T. Nelson, T. H. Emory, T. M. Tuttle, D. Yee and M. Garwood, *Radiology*, 2004, **233**, 424–431.
18 M. Law, S. Cha, E. A. Knopp, G. Johnson, J. Arnett and A. W. Litt, *Radiology*, 2002, **222**, 715–721.
19 D. J. Manton, A. Chaturvedi, A. Hubbard, M. J. Lind, M. Lowry, A. Maraveyas, M. D. Pickles, D. J. Tozer and L. W. Turnbull, *Br. J. Cancer*, 2006, **94**, 427–435.
20 J. Kurhanewicz, D. B. Vigneron and S. J. Nelson, *Neoplasia*, 2000, **2**, 166–189.
21 A. M. Groves, T. Win, S. B. Haim and P. J. Ell, *Lancet Oncol.*, 2007, **8**, 822–830.
22 N. Shinoura, M. Nishijima, T. Hara, T. Haisa, H. Yamamoto, K. Fujii, I. Mitsui, N. Kosaka and T. Kondo, *Radiology*, 1997, **202**, 497–503.
23 T. Hara, N. Kosaka, N. Shinoura and T. Kondo, *J. Nucl. Med.*, 1997, **38**, 842–847.
24 J. Klein, A. Koppen and K. Loffelholz, *Neurochem. Int.*, 1998, **32**, 479–485.
25 J. Klein, A. Koppen and K. Loffelholz, *J. Neurochem.*, 1991, **57**, 370–375.
26 J. Klein, A. Koppen and K. Loffelholz, *J. Neurochem.*, 1990, **55**, 1231–1236.
27 R. Katz-Brull, R. Margalit, P. Bendel and H. Degani, *Mag. Reson. Mater. Phys. Biol. Med.*, 1998, **6**, 44–52.
28 K. Kanamori and B. D. Ross, *Magn. Reson. Med.*, 1999, **41**, 456–463.
29 K. Kanamori and B. D. Ross, *Biochem. J.*, 1993, **293**(Pt 2), 461–468.
30 G. M. Abragam A, *Rep. Prog. Phys.*, 1978, **41**, 395–467.
31 J. H. Ardenkjaer-Larsen, B. Fridlund, A. Gram, G. Hansson, L. Hansson, M. H. Lerche, R. Servin, M. Thaning and K. Golman, *Proc. Natl. Acad. Sci. U. S. A.*, 2003, **100**, 10158–10163.
32 F. A. Gallagher, M. I. Kettunen, S. E. Day, D. E. Hu, J. H. Ardenkjaer-Larsen, R. Zandt, P. R. Jensen, M. Karlsson, K. Golman, M. H. Lerche and K. M. Brindle, *Nature*, 2008, **453**, 940–943.
33 K. Golman and J. S. Petersson, *Acad. Radiol.*, 2006, **13**, 932–942.
34 K. Golman, R. I. Zandt, M. Lerche, R. Pehrson and J. H. Ardenkjaer-Larsen, *Cancer Res.*, 2006, **66**, 10855–10860.
35 A. Comment, B. van den Brandt, K. Uffmann, F. Kurdzesau, S. Jannin, J. A. Konter, P. Hautle, W. T. H. Wenckebach, R. Gruetter and J. J. van der Klink, *Concepts Magn. Reson., Part B*, 2007, **31B**, 255–269.
36 M. L. Zierhut, Y. F. Yen, A. P. Chen, R. Bok, M. J. Albers, V. Zhang, J. Tropp, I. Park, D. B. Vigneron, J. Kurhanewicz, R. E. Hurd and S. J. Nelson, *J. Magn. Reson.*, 2009.
37 A. P. Chen, M. J. Albers, C. H. Cunningham, S. J. Kohler, Y. F. Yen, R. E. Hurd, J. Tropp, R. Bok, J. M. Pauly, S. J. Nelson, J. Kurhanewicz and D. B. Vigneron, *Magn. Reson. Med.*, 2007, **58**, 1099–1106.
38 R. B. van Heeswijk, K. Uffmann, A. Comment, F. Kurdzesau, C. Perazzolo, C. Cudalbu, S. Jannin, J. A. Konter, P. Hautle, B. van den Brandt, G. Navon, J. J. van der Klink and R. Gruetter, *Magn. Reson. Med.*, 2009, **61**, 1489–1493.
39 H. Middleton, R. D. Black, B. Saam, G. D. Cates, G. P. Cofer, R. Guenther, W. Happer, L. W. Hedlund, G. A. Johnson and K. Juvan, *et al.*, *Magn. Reson. Med.*, 1995, **33**, 271–275.
40 R. Sarkar, A. Comment, P. R. Vasos, S. Jannin, R. Gruetter, G. Bodenhausen, H. Hall, D. Kirik and V. P. Denisov, *J. Am. Chem. Soc.*, 2009, **131**, 16014–16015.
41 C. Gabellieri, S. Reynolds, A. Lavie, G. S. Payne, M. O. Leach and T. R. Eykyn, *J. Am. Chem. Soc.*, 2008, **130**, 4598–4599.
42 A. Comment, B. van den Brandt, K. Uffmann, F. Kurdzesau, S. Jannin, J. A. Konter, P. Hautle, W. T. Wenckebach, R. Gruetter and J. J. van der Klink, *Appl. Magn. Reson.*, 2008, **34**, 313–319.
43 T. Ethofer, I. Mader, U. Seeger, G. Helms, M. Erb, W. Grodd, A. Ludolph and U. Klose, *Magn. Reson. Med.*, 2003, **50**, 1296–1301.
44 R. P. Shockley and J. C. LaManna, *Brain Res.*, 1988, **454**, 170–178.
45 L. Darrasse and J. C. Ginefri, *Biochimie*, 2003, **85**, 915–937.
46 K. Golman, J. H. Ardenkjaer-Larsen, J. S. Petersson, S. Mansson and I. Leunbach, *Proc. Natl. Acad. Sci. U. S. A.*, 2003, **100**, 10435–10439.
47 K. Golman, R. in't Zandt and M. Thaning, *Proc. Natl. Acad. Sci. U. S. A.*, 2006, **103**, 11270–11275.
48 F. Kurdzesau, B. van den Brandt, A. Comment, P. Hautle, S. Jannin, J. J. van der Klink and J. A. Konter, *J. Phys. D-Appl. Phys.*, 2008, 41.
49 D. Gelvan, P. Saltman and S. R. Powell, *Proc. Natl. Acad. Sci. U. S. A.*, 1991, **88**, 4680–4684.
50 Y. Miura, A. Hamada and H. Utsumi, *Free Radical Res.*, 1995, **22**, 209–214.

51 H. Li, L. Ma, C. J. Hsia, J. L. Zweier and P. Kuppusamy, *Free Radical Biol. Med.*, 2002, **32**, 712–719.
52 S. M. Hahn, F. J. Sullivan, A. M. DeLuca, C. M. Krishna, N. Wersto, D. Venzon, A. Russo and J. B. Mitchell, *Free Radical Biol. Med.*, 1997, **22**, 1211–1216.
53 M. Terpstra, P. M. Andersen and R. Gruetter, *J. Magn. Reson.*, 1998, **131**, 139–143.
54 R. Gruetter and I. Tkac, *Magn. Reson. Med.*, 2000, **43**, 319–323.
55 M. Garwood and K. Yong, *J. Magn. Reson.*, 1991, **94**, 511–525.
56 L. Vanhamme, A. van den Boogaart and S. Van Huffel, *J. Magn. Reson.*, 1997, **129**, 35–43.
57 A. Naressi, C. Couturier, I. Castang, R. de Beer and D. Graveron-Demilly, *Comput. Biol. Med.*, 2001, **31**, 269–286.
58 S. Cavassila, S. Deval, C. Huegen, D. van Ormondt and D. Graveron-Demilly, *NMR Biomed.*, 2001, **14**, 278–283.